PCCP

View Online
Dynamic Article Links

Cite this: *Phys. Chem. Chem. Phys.*, 2011, **13**, 11340–11350

www.rsc.org/pccp

PAPER

Nitrogen/gold codoping of the TiO_2(101) anatase surface. A theoretical study based on DFT calculations

Yanaris Ortega,[a] Norge Cruz Hernández,[b] Eduardo Menéndez-Proupin,[c] Jesús Graciani[a] and Javier Fdez. Sanz*[a]

Received 9th November 2010, Accepted 19th April 2011
DOI: 10.1039/c0cp02470h

The interaction between implanted nitrogen atoms, adsorbed gold atoms, and oxygen vacancies at the anatase TiO_2(101) surface is investigated by means of periodic density functional theory calculations. Substitutional and interstitial configurations for the N-doping have been considered, as well as several adsorption sites for Au adatoms and different types of vacancies. Our total energy calculations suggest that a synergetic effect takes place between the nitrogen doping on one hand and the adsorption of gold and vacancy formation on the other hand. Thus, while pre-implanted nitrogen increases the adsorption energy for gold and decreases the energy required for the formation of an oxygen vacancy, pre-adsorbed gold or the presence of oxygen vacancies favors the nitrogen doping of anatase. The analysis of the electronic structure and electron densities shows that a charge transfer takes place between implanted-N, adsorbed Au and oxygen vacancies. Moreover, it is predicted that the creation of vacancies on the anatase surface modified with both implanted nitrogen and supported gold atoms produces migration of substitutional N impurities from bulk to surface sites. In any case, the most stable configurations are those where N, Au and vacancies are close to each other.

1. Introduction

Anatase is one of the most common titanium oxide polymorphs, widely used in many applications including heterogeneous catalysis, photocatalysis, dye sensitized solar cells, white pigments and electronic devices.[1] As a photocatalyst it is inexpensive, nontoxic, chemically inert, resistant to photo-corrosion and has a thermal and mechanical stability.[2–4] Special attention has been given to this material since the discovery of hydrogen production *via* photoinduced water splitting on this kind of semiconductor.[5] The primary drawback of this oxide is the large optical gap (3.2 eV),[12] which restricts the photocatalytic activity to the ultraviolet light region that carries approximately 4% of the solar radiation at the Earth's surface. The main strategy towards achieving activity under visible light is to create a donor or an acceptor level in the band-gap,[6] by means of doping and/or adsorption of transition metals such as Cr, Au or Ni,[1,7,8] nonmetals (C, N, B, S),[9–12] and creation of vacancies in the structure.[13,14]

It has been found that doping with transition metals leads to positive and negative consequences on the photocatalytic properties. Among the negative consequences, one can mention an increase of charge-carrier recombination, thermal instability and no noticeable change in the band gap of TiO_2,[15–17] the improvement in visible light absorption coming from d–d electronic transitions within the metal dopants and not from a band gap narrowing of the oxide. Vittadini *et al.*[16] studied theoretically the adsorption of Au_n (n = 1, 2, 3) cluster on the stoichiometric and the reduced (101) surface of anatase. They observed that the gold particle is preferentially coordinated to the anionic sites, and such interaction must increase with the cluster size. Meanwhile, the adsorption on the reduced surface indicates the affinity of the metal to stay in the vacancy sites.

To date, non-metal doped materials have been further studied because they are one of the most promising materials that have been synthesized. Since the work of Asahi *et al.*,[9] nitrogen doping has been widely studied due to the fact that it can significantly improve the photocatalytic behavior of the oxide. They showed how a gap narrowing takes place due to the mixture of N 2p and O 2p bands. Di Valentin *et al.*[18,19] have studied the nitrogen implantation in interstitial and substitutional positions, and the interaction of this implanted N with the oxygen vacancies. Finazzi *et al.*[19] observed that substitutional N prefers sub-surface three-coordinated sites, while interstitial N is located in surface layers preferably. They showed that the implantation of nitrogen modifies the electronic structure of the surface, resulting in localized states at the top of the valence band and within the gap as well as reduction of

[a] *Departamento de Química Física, Facultad de Química, Universidad de Sevilla, E-41012 Sevilla, Spain. E-mail: sanz@us.es*
[b] *Departamento de Física Aplicada I, Escuela Universitaria Politécnica, Universidad de Sevilla, E-41011 Sevilla, Spain*
[c] *Departamento de Física, Facultad de Ciencias, Universidad de Chile, Santiago, Chile*

the optical absorption threshold. The main disadvantage of N doping is the relatively low concentration of dopant (2%) that can be achieved,[20] because N is unstable with respect to formation of gaseous N_2.[21] Nevertheless, such an escape can be partially avoided by the presence of vacancies, because the total energy can be reduced, thanks to electronic transfer from the occupied higher energy oxygen vacancy levels to the empty lower energy implanted N 2p band, stabilizing the implanted N by closing its electronic shell, and allowing lower energy electronic configuration of the system.[22] Some authors[23,24] have found the fact that N doping favors the creation of vacancies and a relationship between the presence of oxygen vacancies and the surface reactivity.

A further step is the combination of non-metal doping with adsorption of transition metals. In an experimental study, Sakthivel *et al.*[25] have recently examined the effects of the presence of vacancies in the anatase $TiO_{2-x}N_x$ on the supported Au. They have found an increment of the catalytic activity with respect to the stoichiometric system. Some experiments[26–28] confirm that the TiO_2 surface properties dramatically affect the catalytic activity, which is related to the metal–support interaction, and consequently to the stability of deposited gold particles and the final gold dispersion. Although gold deposition at low coverage has not yet been published for anatase $TiO_{2-x}N_x$ on the supported Au, its high catalytic activity has been demonstrated, both experimentally and theoretically, for other titanium oxide surfaces.[29,30] It has also been shown that to take into account the presence of water on the surface, as normally takes place in the atmosphere or as a reactant, is crucial for a better understanding of how anatase–TiO_2 and γ-alumina exhibit catalytic activity[31] as well as the growth mechanism of a metal deposited on another surface, such as α-alumina.[32] However, in order to reduce the complexity of the system, only anhydrous case has been treated in this paper.

As far as we know, there is not any study reported in which the interaction between the anionic vacancies, adsorbed gold atoms and implanted nitrogen into the anatase surface has been investigated. A theoretical paper with experimental support on the electronic structure and surface properties induced by the aforementioned modifiers, as well as their effects in the catalytic activity, has been previously published by our group for rutile.[33] It was shown in this work that the introduction of such surface modifiers is able to stabilize the system due to charge transfers, improving at the same time the catalytic behavior of the system, suggesting that the $Au/TiO_{2-x}N_y$ system is more active than Au/TiO_2 for the water gas shift reaction.

In this article, we study the structural, energetic, and electronic properties of the anatase(101) surface under conditions of N doping, Au adsorption and the presence of oxygen vacancies. The periodic density functional theory (DFT) has been used throughout this research. We study: (i) the N–Au and N–Au-vacancy interactions, and (ii) the capability of these species to improve the visible light absorption and the photocatalytic behavior of the system.

2. Computational details

DFT-periodic calculations were carried out using the Vienna *Ab initio* Simulation Package (VASP)[34–36] with the projector augmented wave method (PAW).[37] The calculations have been performed within the generalized gradient approximation (GGA) and the periodic plane-wave approach using the Perdew–Burke–Ernzerhof (PBE) exchange–correlation functional.[38,39] In the $TiO_{2-x}N_y$, due to the presence of the paramagnetic N atoms, spin-polarized DFT calculations have been performed. For systems containing both N and Au species, having even number of electrons, we have made non-spin-polarized calculations for all structures. In order to check that the system is really non spin-polarized in some typical cases (N and Au atoms close one to the other and another case in which they are far away; in both, the reduced and non-reduced surface), spin-polarized calculations were also performed but no noticeable difference in structural geometry and energy was found. The valence states that are explicitly included in the calculation are 3p, 3d and 4s for Ti atoms; 2s and 2p for O and N atoms; together with 5d and 6s states for the Au atoms; while the core electrons are kept at frozen states. A kinetic energy cutoff of 500 eV was found necessary to satisfactorily describe the system and to reproduce the relative energies of implanted N impurities obtained by Finazzi *et al.*[19]

The anatase structure is characterized by the tetragonal space group $I4/amd$.[2] A number of $4 \times 4 \times 2$ k-points mesh for anatase bulk (12 atoms) are enough to reach negligible changes in the optimized cell parameters and energy. The bulk lattice parameters obtained were $a = 3.789$ Å, $c = 9.486$ Å which are within 0.2% of the experimental values ($a = 3.782$ Å, $c = 9.502$ Å).[40]

The (101) surface was modeled as a periodically repeated slab inside a supercell. We think that this model is adequate to represent the interaction of the impurities and their experimental concentrations. The supercell contains 72 atoms (24 Ti and 48 O) and its dimensions are 1×2 in the $[10\bar{1}]$ and [010] directions, respectively. In the direction [101], the slab has three Ti_8O_{16} layers (there are six atomic layers per each Ti_8O_{16} layer) and a vacuum of 9 Å (Fig. 1).[19] The coordinates of the atoms in the bottom atomic layer were kept fixed while the rest of the atoms were allowed to relax. The Brillouin zone was sampled using a $2 \times 2 \times 1$ grid of k-points using the Monkhorst–Pack method.[41] The Hellmann–Feynman

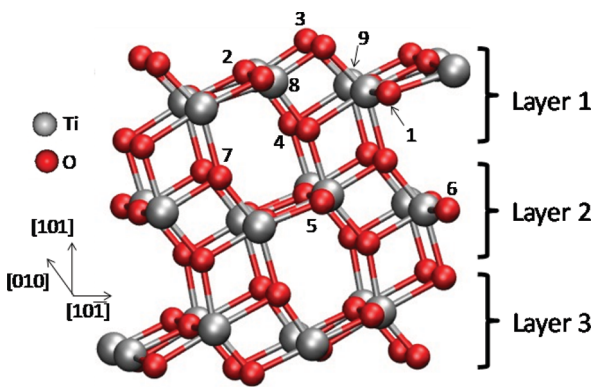

Fig. 1 General view of the anatase(101) surface. The labeling for the substitutional sites is: (1) s3d (s-3c-down), (2) s3u (s-3c-up), (3) s2b (s-2c-bridging), (4) b3sb (b-3c-sub-bridging), (5) b3u (b-3c-up), (6) b3d (b-3c-down), (7) b3b (b-3c-bridging), (8) Ti-5c, (9) Ti-6c.

theorem was used to calculate forces of the ions through partial derivatives of free energy with respect to the atomic position. A Gaussian smearing with k_BT = 0.1360 eV has been applied to the density of states to avoid convergence problems, while keeping the fictitious entropy contribution to the free energy at levels smaller than 1 meV per atom. Structural minimizations were performed using a conjugated gradient technique in which the iterative relaxation of atomic positions was stopped when the change in the total energy between successive steps was less than 0.001 eV. With this criterion, forces on the atoms were generally less than 0.1 eV Å^{-1}. The dipolar correction was not normally applied in our calculations, but it was used in the case of the most stable case for each model and no perceptible changes were obtained. The density of states (DOS) for the relaxed structures were obtained sampling the Brillouin zone and a 4 × 4 × 2 grid interpolated using the tetrahedron method with Blöchl corrections.[42,43] As a special test, in order to investigate the electronic properties of the surface after nitrogen implantation, gold deposition and vacancy creation; one of the most stable systems was re-optimized by using the GGA + U approximation introduced by Dudarev *et al.*,[44] where the *U* value is 5.5 eV as proposed in ref. 45. After that, the DOS was also obtained with the aim of demonstrating the localization effect on the 3d Ti atom levels.

The implantation of N atoms in the structure was performed on both substitutional and interstitial positions. To identify the non-equivalent substitutional implantation sites, we used a nomenclature similar to that used by Finazzi *et al.*:[19] the labels "s-" or "b-" indicate a surface and bulk (subsurface) site, respectively; "*n*-" (*n* = 2 or 3) indicates the number of Ti atoms bound to N atoms, whereas "u", "d" and "b" indicate outward, inward and bridging positions, respectively. For example, the site "s2b" (s-2c-bridging) is a surface position that bridges two Ti atoms. All the substitutional sites considered are shown in Fig. 1. Besides, five non-equivalent interstitial N doping sites have been studied (Fig. 2), each denoted by the type and the relative position of the closer O atom. In this way, the type of oxygen atom is defined by using the same nomenclature rule as in the case of substitution, but

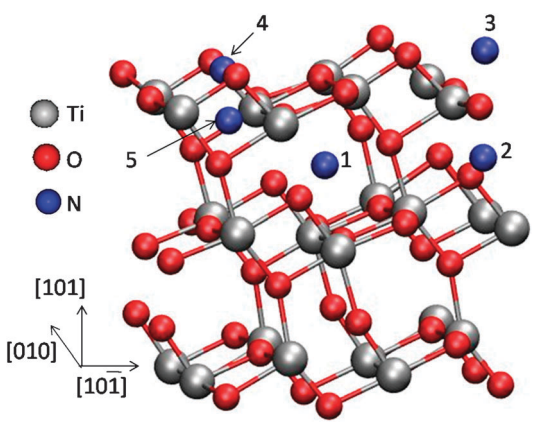

Fig. 2 The labeling of the five interstitial sites: (1) b3b (b-3c-bridging), (2) s3d_above (s-3c-down_above), (3) s3d_below (s-3c-down_below), (4) s2b_between (s-2c-bridging_between), (5) s2b_below (s-2c-bridging_below).

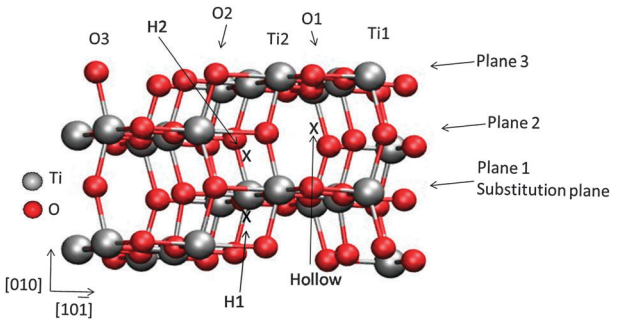

Fig. 3 Top view of the slab model showing the adsorption sites for Au on the (101) anatase surface.

other key word has been added: above, between and below; to define that the N atom is located above, between and below the oxygen atoms, respectively (note that these words are used only for interstitial N doping cases). Thus, s2b_below means that the N atom is located below an oxygen atom at the s2b position.

The adsorption sites studied for the gold atoms are shown in Fig. 3. We have considered eighteen adsorption sites: three possible surface positions labeled H1, H2 and Hollow, and fifteen on the outermost atoms. These atoms are identified as follows: the supercell has three non-equivalent planes (planes 1, 2, and 3) perpendicular to the surface, and each plane has two Ti atoms and three O atoms in the outermost layer. For example, "b3b-O2p1" stands for a configuration where the substitutional nitrogen is in a b3b site and a gold atom is deposited on the oxygen 2 that belongs to plane 1 (O2p1), while in the "s2b_below-O2p3" configuration, the interstitial nitrogen is situated on the s2b_below position and a gold atom is deposited over the oxygen 2 that belongs to plane 3 (O2p3). Take into account that planes 1 and 3 are equivalent in a stoichiometric surface, but the symmetry is broken by the presence of an impurity. Special attention needs the case where the gold atom is deposited on top of the nitrogen atom. In such case, the key word "topN" is used in order to define the position of the adsorbed metallic atom. For instance, "b3b-topN" indicates that the gold atom has been located on top of the nitrogen atom substituted in the position b3b.

After deposition of gold atoms, oxygen vacancies have been created in the first and second layer; we follow the same labeling that of the substitutional N sites to identify the vacancy positions. First, the position of the nitrogen (substitutional or interstitial) is indicated, followed by the gold atom and finally the vacancy position. For example, s3d_below-O2p3-b3u means that the interstitial nitrogen is situated on the s3d_below position, a gold atom is adsorbed over the oxygen 2 that belongs to plane 3 (O2p3) and the vacancy has been created in a b3u site.

3. Results and discussion

3.1 Substitutional N doping

3.1.1 $Au/TiO_{2-x}N_x$ system. Previous studies on the substitutional N doping on anatase have shown that nitrogen prefers substitutional subsurface positions rather than surface

sites, specifically, the b3b site, in agreement with the tendency of the N atoms to be at 3-fold coordinate positions.[18,19] However, the relative energies reported are small, suggesting that the N atoms can be found randomly distributed in the lattice.

The implantation energy taking as reference $N_{2(g)}$ is defined for the reaction:

$$\frac{x}{2}N_{2(g)} + TiO_2 \rightarrow TiO_{2-x}N_x + \frac{x}{2}O_{2(g)}$$

as

$$E_{imp}^{N} = E(TiO_{2-x}N_x) + \tfrac{1}{2}E(O_{2(g)}) - \tfrac{1}{2}E(N_{2(g)}) - E(TiO_2)$$

where $E(TiO_2)$, $E(TiO_{2-x}N_x)$, $E(N_{2(g)})$ and $E(O_{2(g)})$ are the bare TiO_2, substitutional-N-doped surface, the molecular nitrogen and oxygen energies, respectively.

According to the implantation energies calculated, E_{imp}^{N}, Table 1, all sites considered are thermodynamically unfavorable for the substitution of oxygen atoms by nitrogen from molecule $N_{2(g)}$. These results show us an endothermic process because the molecule $N_{2(g)}$ has a very high binding energy. Graciani *et al.*[22] studied the implantation by adsorption, substitution and in vacancies of N into the rutile TiO_2(110) surface. As in the anatase surface, they found that the substitution starting from the $N_{2(g)}$ molecule was also an endothermic process. It was almost equally probable in all sites, except in the bridging position, the second layer being more stable than the superficial layers. The implantation energies reported for the rutile surface and our results suggest that the implantation is more likely in rutile than in anatase surface.

To study the localization–delocalization effects of the gold adsorption on the nitrogen doped surface, we selected the most stable configuration (b3b) and the case when the N atom is in the outer layer bonding directly to Au (s2b). The adsorption process and the energy necessary to adsorb the metallic atom on the surface can be represented according to the following formulae:

$$TiO_{2-x}N_x + Au \rightarrow Au/TiO_{2-x}N_x$$

$$E_{ads} = E(Au/TiO_{2-x}N_x) - E(TiO_{2-x}N_x) - E(Au)$$

where $E(Au/TiO_{2-x}N_x)$ and $E(Au)$ are the energies of the adsorbed gold on the N-doped surface and the isolated gold atom, respectively. The energies thus obtained correspond to Au coverage of $\theta = \frac{1}{4}$, and are reported in Table 2. Compared with the value estimated for the interaction with the bare surface (−0.39 eV),[16] it clearly appears that the presence of nitrogen atoms on the anatase network leads to a much stronger interaction. If we compare now these values with the structural parameters reported in Table 3, we can see that the higher the N–Au interaction and direct bonding between them, the higher the adsorption energies reached. The fact that the gold atom tends to interact with anions rather than cations can be explained by a change of its oxidation state due to an electron transfer from the metal towards the support; which is discussed in Section 3.3. The energy values suggest that the largest adsorption energy is achieved when the gold atom is on top of the substituted nitrogen on the surface bridging position, *i.e.*, s2b-topN (Fig. 4a). Taking into account the previous results, we can expect a migration of the N located into the inner layers of the anatase lattice toward the surface to interact with adsorbed gold atoms. The larger adsorption energy of $Au/TiO_{2-x}N_x$(s2b) overcompensates the higher relative energy of the supporting surface s2b compared with b3b, leading to formation of the complex $Au/TiO_{2-x}N_x$(s2b).

Graciani *et al.* studied this interaction in the rutile(110) surface and observed a similar behavior.[33] Typical Au adsorption energies on the stoichiometric rutile surface are −0.29, −0.27 and −0.38 eV in anionic, cationic and O–Ti positions,[46] respectively; while this value increases to −2.55 eV on the N-modified rutile surface, when the Au atom is adsorbed on top of N_{ip} (in-plane nitrogen). The comparison of Table 2 and the adsorption energy when the Au atom is adsorbed on anionic and cationic sites on the bare anatase surface (−0.33 and −0.39 eV, respectively)[16] and on N–TiO_2 (−2.72 eV) suggests that the presence of nitrogen atoms

Table 1 Energies (eV) for substitutional N implantation E_{imp}^{N} into the stoichiometric TiO_2(101) anatase surface

Implant. sites	E_{imp}^{N}	Relative energies
b3b	**4.92**	**0.0**
b3d	5.07	0.15
b3sb	5.05	0.13
b3u	5.10	0.18
s2b	5.16	0.24
s3d	5.06	0.14
s3u	5.18	0.26

Table 2 Adsorption energies (eV) of Au atoms deposited at different sites on the $TiO_{2-x}N_x$ surface. Unstable positions are shown by "—"

	Plane 1		Plane 2		Plane 3	
Adsorption sites	b3b	s2b	b3b	s2b	b3b	s2b
O1	—	**−2.72(topN)**	—	—	−1.00	−1.07
O2	−1.57	—	−1.00	—	—	−1.39
O3	−1.86	−1.82	−1.38	−1.36	—	−1.87
Ti1	**−2.09**	—	—	—	−1.26	−1.26
Ti2	—	—	−1.26	−1.2	—	—
Channels						
Hollow	**−2.00**	**−2.75**				
H1	−1.77	—				
H2	—	—				

Table 3 Au–N bond distances (Å) for Au adsorbed on different sites in the $TiO_{2-x}N_x$ surface

	Plane 1		Plane 2		Plane 3	
Adsorption sites	b3b	s2b	b3b	s2b	b3b	s2b
O1	—	**1.94(topN)**	—	—	6.45	5.11
O2	5.74	—	6.55	—	—	4.24
O3	5.87	5.08	6.99	5.38	—	4.24
Ti1	**4.47**	—	—	—	5.92	4.31
Ti2	—	—	7.18	4.19	—	—
Channels						
Hollow	**5.08**	**2.03**				
H1	5.77	—				
H2	—	—				

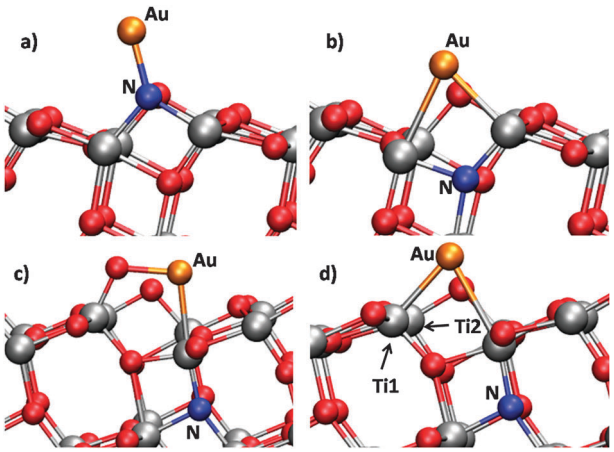

Fig. 4 Geometries of the most stable configurations of Au deposited on substitutional N-doped anatase with and without vacancies: (a) s2b-topN, (b) after removing an oxygen: s2b-topN-b3sb, (c) b3b-Ti1p1 and (d) after removing an oxygen: b3b-Ti1p1-s2b.

tremendously increases the metal–support interaction in both surfaces, the effect being even higher in the anatase(101) surface.

3.1.2 Oxygen vacancies on the $Au/TiO_{2-x}N_x$ system. The reactivity of this type of oxides is largely influenced by the presence of oxygen vacancies. Most of the articles in the literature reported so far are focused on bridging oxygen vacancies. So, to examine the influence of other kinds of vacancies in the N-modified anatase supported Au and the interaction between species (N, Au and vacancy V^o) is an interesting issue. To this aim we consider models in which one oxygen atom is removed from one of the first two layers. In order to evaluate the direct and indirect interaction between the impurities, we choose the most stable configurations found in the previous section, s2b-topN and b3b-Ti1p1 (Fig. 4a and c).

The reaction for a vacancy formation on $Au/TiO_{2-x}N_x$ can be written as:

$$Au/TiO_{2-x}N_x \rightarrow Au/TiO_{2-x-y}N_x + \frac{y}{2}O_{2(g)}$$

The vacancy formation energy by removing one oxygen atom from one neutral surface super-cell $Au/TiO_{2-x}N_x$ is calculated by:

$$E_{fv} = E(Au/TiO_{2-x-y}N_x) + \mu_0 - E(Au/TiO_{2-x}N_x)$$

where $E(Au/TiO_{2-x-y}N_x)$ indicates the energy of the system with a vacancy in the super-cell surface and μ_0 is the oxygen chemical potential[47] with $\mu_0 = \frac{1}{2}E(O_2) + \mu'_0$. $E(O_2)$ is the total energy of an isolated oxygen molecule in a triplet state, and $\mu'_0 = \frac{1}{2}kT\ln(p/p_0)$.[48]

Fig. 5 illustrates the dependence of the formation energy *vs.* oxygen pressure at 700 K temperature, while Table 4 (left and center) shows the formation energies under the particular case of oxygen-rich conditions $(p/p_0) = 1$ for different sites of the vacancy. The energy values exhibit a clear tendency: when the nitrogen is located on subsurface layers, the creation of vacancies is favored at the surface, as might be observed in the most stable configurations b3b-Ti1p1-s2b and s2b-topN-b3sb. In b3b-Ti1p1-s2b (Fig. 4d), the metallic atom is adsorbed on the bridging vacancy. In the case of the s2b-topN-b3sb

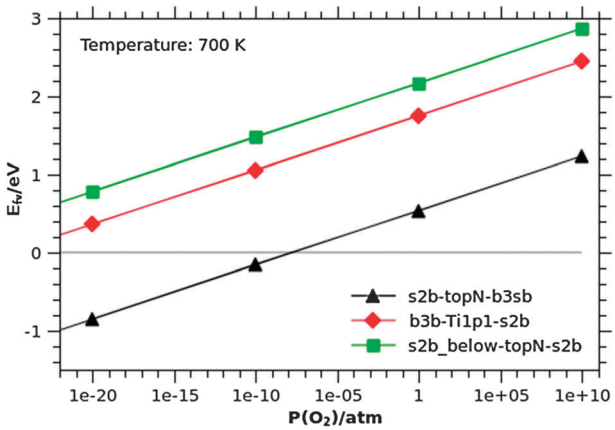

Fig. 5 Stability diagram for the various surface N-doped anatase on gold deposited models considered for oxygen vacancy at 700 K temperature and a wide range of pressures.

Table 4 Energy of vacancy formation, E_{fv} (eV), at the $Au/TiO_{2-x}N_x$ and Au/TiO_2N_x surfaces

	Substitutional		Interstitial
V^o sites	b3b-Ti1p1	s2b-topN	s2b_below-topN
b3b	4.37	4.23	3.68
b3sb	3.64	**0.54**	2.64
b3u	5.00	4.81	4.87
b3d	4.89	4.83	4.95
s2b	**1.75**	4.31	**2.17**
s3d	3.26	4.88	2.79
s3u	2.74	3.29	3.33

configuration (Fig. 4b), the bridging nitrogen atom migrates to a subsurface position (the position of the vacancy b3sb) and the vacancy occupies the bridging sites to interact with both gold and nitrogen atoms simultaneously. The observation of vacancy migration from bulk to surface has been reported in previous experimental works.[22,49–51] It is worth noting that the gold atom prefers to interact with the Ti atoms, suggesting that Au atoms are neutral or negatively charged, as we will analyze in Section 3.3. The high energy value found for the s2b-topN-b3sb configuration is due to the fact that the gold atom binds to the nearest Ti atoms and there is a direct interaction among the impurities. Indeed, the shorter the distance between the vacancy and one of the impurities (gold or/and nitrogen), the larger the adsorption energy is.

Calculation of vacancy energies in TiO_2 is a quite controversial issue as the obtained values significantly depend on the model, size and thickness of the slab, as well as on computational settings.[52,58] In the case of anatase, the lowest values we have found are 3.80 and 3.66 eV for bridging surface and subsurface sites, respectively. These are in agreement with those recently reported by Cheng and Selloni.[53] This energy is reduced to 2.37 eV when the N is implanted, *i.e.* a lowering of 1.29 eV. On the other hand, when an Au atom is deposited on the undefective surface, the vacancy formation energy diminishes to 1.83 eV; thus, the lowering in this case, 1.83 eV, is larger than for the N-doped surface. Finally, removing a bridging oxygen atom from the system, when both Au and N are present, only costs 1.75 eV. It means that the simultaneous

presence of impurities favors the creation of vacancies at the surface even though the effect is not additive since there is a competition between N and Au to stabilize the vacancy electrons. The creation of vacancy is favored according to the order: $Au/TiO_{2-x}N_x > Au/TiO_2 > TiO_{2-x}N_x > TiO_2$. It should be noticed that in the case of model s2b-topN (Fig. 4a), the stabilization is much larger, with a vacancy energy formation of 0.54 eV although it corresponds to a structure in which the vacancy initially created at the subsurface is filled by the N atom, and the gold atom migrates to fill the hole (Fig. 4b).

3.2 Interstitial N doping

3.2.1 Au/TiO_2N_x system. The interstitial implantation of the nitrogen atom was studied by Finazzi *et al.*[19] They reported that the interstitial nitrogen neatly prefers to occupy positions on superficial layers, in contrast with the substitutional case, where N can be found randomly distributed in the lattice. Also, while substitutional configurations are not accompanied by appreciable structural changes, the presence of the interstitial nitrogen leads to significant variations in the local geometry and formation of N–O species, with bond distances in the 1.3–1.4 Å range (the experimental bond distance of the NO molecule is 1.17 Å). The optimized geometry of the most stable configuration, s2b_below, is depicted in Fig. 6a, in which the presence of a N–O species is clearly seen. This is in contrast with what was found in rutile, where the interstitial N is stable in subsurface positions and therefore it is common to find N_2 into the channels of the material.[22,54]

To study the implantation process and its stability for the considered models we examine the insertion of a nitrogen atom from $N_{2(g)}$ in the lattice. It can be represented as:

$$\frac{x}{2}N_{2(g)} + TiO_2 \rightarrow TiO_2N_x$$

$$E^{N}_{imp} = E(TiO_2N_x) - \tfrac{1}{2}E(N_{2(g)}) - E(TiO_2)$$

where $E(TiO_2N_x)$ is the energies of the interstitial-N-doped system.

The results, shown in Table 5, suggest that the implantation taking as reference the nitrogen molecule is an endothermic process whatever the site is, and the superficial positions have marked stability with respect to sub-surface cases. As already commented for the substitutional case, due to the large bond strength in the $N_{2(g)}$ molecule, it is less likely that it dissociates and adsorbs one of the atoms in the structure, none of the new bonds formed with the surface is able to compensate for the breaking of the strong N–N bond. The same behavior is observed in the rutile phase. The implantation process through the interstitial mechanism is favored with respect to the substitutional one, since E^{N}_{imp} are in the range of 4.92 to 5.18 eV for the substitutional models and 2.71 to 4.47 eV for the interstitial case. Graciani *et al.* studied the adsorption of N atoms in different sites on the surface and interstitial.[22] The most stable site to adsorb is on top of bridging oxygen forming NO like species, while the less stable position, by 0.35 eV, is for that occupying an interstitial position into the rutile channels. If we compare the implantation or adsorption energies, and in particular the most stable configurations (s2b_below and s2b_between) where the N migrates to the surface to adsorb on bridging oxygen, it is worth remarking that it is easier to adsorb or implant N at interstices on anatase than on rutile. On the other hand, the formation of N_2 is an exothermic process ($E^{N}_{esc} = E^{N}_{imp}$), and therefore it is likely that implanted N evolves as $N_{2(g)}$ when a N atom finds each other. Thus, the N implantation *via* interstices would proceed at low concentrations.

Table 5 Energies (eV) for interstitial N implantation E^{N}_{imp} into the stoichiometric TiO_2(101) anatase surface

Implantation sites		E^{N}_{imp}	Relative energy
b3b		4.47	1.75
s2b	Below	2.71	0.0
	Between	3.13	0.41
s3d	Above	4.44	1.72
	Below	3.94	1.22

Finazzi *et al.*[19] obtained the stability for the interstitial and substitutional N doped TiO_2 in a wide range of O_2 pressures and 700 K. They observed that under oxygen-poor conditions to substitute N atoms is more likely. But, moving toward oxygen-rich conditions the presence of interstitial species is the most stable in a wide range of oxygen chemical potentials. They compared with previous results[55] and reported that the stability range of interstitial impurities into the surface is larger than in bulk.

Once we have reviewed the general features of interstitial doping on the anatase(101) surface, we examine the adsorption of the gold atom on the interstitial nitrogen implanted surface. To this aim we have chosen the most stable situation in interstitial doping, s2b_below. The adsorption energies for the Au atom on the surface were calculated according to the following formulae:

$$TiO_2N_x + Au \rightarrow Au/TiO_2N_x$$

$$E_{ads} = E(Au/TiO_2N_x) - E(TiO_2N_x) - E(Au)$$

where $E(Au/TiO_2N_x)$ is the Au-supported interstitial-N-modified surface. In this study only one gold atom is adsorbed, thus Au coverage is $\theta = 0.25$.

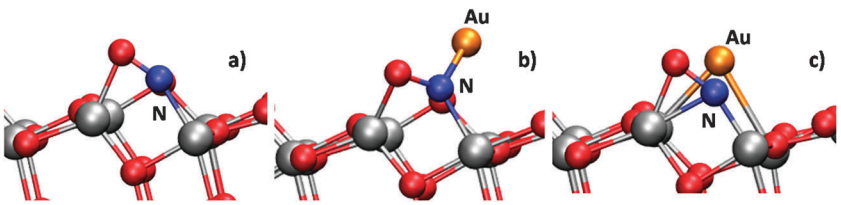

Fig. 6 Geometries of the most stable configurations: (a) s2b_below, (b) s2b_below-topN, and (c) s2b_below-topN-s2b.

Table 6 Adsorption energies (in eV) for Au atoms deposited at different sites on the TiO_2N_x surface, s2b_below model

	Planes		
Adsorption sites	1	2	3
O1	−0.75	—	—
O2	−0.2	−0.38	−0.18
O3	−0.42	—	−0.38
Ti1	−0.21	—	—
Ti2	−0.77	—	—
topN	**−1.15**		
Channels			
Hollow	**−1.2**		
H1	—		
H2	—		

Table 6 shows the relative and calculated adsorption energies for the different sites considered. As shown, the preferred sites are on top of the implanted N atom (Fig. 6b) and the hollow site, in which the Au atom is located between the N atom and a bridging O. The energy values indicate that the shorter the N–Au bond distance (see Table 7 for the structural parameters), the larger the interaction energies. This trend is similar to that found for the substitutional case, and due to an ionic interaction as it will be discussed in Section 3.3.

In summary, doping the anatase surface with nitrogen lowers the Au adsorption energy from −0.39 eV (clean surface)[16] to −2.75 eV (substitutional N) and −1.2 eV (interstitial N) showing that N implantation increases the metal–support interaction. The lower value estimated for the interstitial case is likely related to the lower binding capabilities of N atoms already involved in the formation of NO species.

3.2.2 Oxygen vacancies on the Au/TiO_2N_x system. Let us move now to the role of vacancies in these systems and analyze how its presence disturbs the interaction between nitrogen, gold and the support. To this aim we have considered all kinds of possible oxygen vacancies within the first two layers, taking as starting structure model s2b_below-topN (Fig. 6b). The reaction for a vacancy formation on Au/TiO_2N_x can be written as:

$$Au/TiO_2N_x \rightarrow Au/TiO_{2-y}N_x + \frac{y}{2}O_{2(g)}$$

Table 7 Au–N bond distances (Å) at different Au adsorption sites on the TiO_2N_x (s2b_below)

	Planes		
Adsorption sites	1	2	3
O1	5.21	—	—
O2	3.12	5.78	4.97
O3	3.34	—	4.22
Ti1	2.84	—	—
Ti2	1.99	—	—
topN	**2.04**		
Channels			
Hollow	**2.05**		
H1	—		
H2	—		

In a similar way as in the case of substitutional implant, the vacancy formation energy here is calculated by:

$$E_{fv} = E(Au/TiO_{2-y}N_x) + \mu_0 - E(Au/TiO_2N_x)$$

where $E(Au/TiO_{2-y}N_x)$ is the energy of the system with a vacancy at the supported-Au interstitial-N-modified surface. To remove one oxygen atom in the first two layers corresponds to a concentration of 6.25%.

Fig. 5 demonstrates the variation of the formation energy *vs.* oxygen pressure at 700 K temperature, while Table 4 (right) shows the formation energies under oxygen-rich conditions $p/p_0 = 1$ for different sites of the vacancy. As can be seen, the preferred configurations are those in which the coinage metal atom is close to the vacancy V^o for any pressure conditions (*i.e.* the three lines are parallel for any pressure); in particular, in the most stable geometry, s2b_below-topN-s2b, E_{fv} = 2.17 eV, the gold atom fills the vacancy and binds to the nearest Ti center (Fig. 6c). In general, the smaller the Au–V^o and N–V^o distances, the higher the stability of the structure.

Let us now compare once again the effects on the vacancy energies of interstitial N and Au. When a N atom is at the interstices the vacancy formation energy drops from 3.80 to 3.02 eV, and when a gold atom is present this energy lowers again to 2.17 eV, showing that if we take as reference the vacancy energy formation of N-implanted anatase, the presence of gold favors the creation of vacancies. This result agrees with that observed for substitutional N doping and is in contrast with the one found for the rutile TiO_2(110) surface, where the presence of gold on the surface hampers the creation of oxygen vacancies.[33]

3.3 Electronic structure

To get an insight into the electronic changes that underlie the energetic effects observed in the above subsections, the electronic structure, in terms of DOS and Bader charges,[56] will be discussed. Perfect anatase TiO_2 is a semiconductor where the formal oxidation states of oxygen and titanium are O^{2-} and Ti^{4+}, respectively. Its valence band is mainly formed of O 2p states and it is completely filled, while the conduction band is essentially composed by Ti 3d states.[57,58] The experimental band gap energy is approximately 3.2 eV, but LDA and GGA give values of 2.45–2.50 eV, approximately.[4] This underestimation of the gap is well known and mainly attributed to the incomplete cancellation of the self-interaction of the pure GGA exchange/correlation functionals.[58] The total DOS for the clean TiO_2 anatase surface is drawn at the bottom of Fig. 7, and clearly shows this underestimation.

The implant procedures can be formally written as:

$$xN + Ti(O^{2-})_2 \rightarrow Ti(O^{2-})_{2-x}(N^{2-})_x + \frac{x}{2}O_2 \quad \text{substitutional implant}$$

$$xN + Ti(O^{2-})_2 \rightarrow Ti(O^{2-})_2(N)_x \quad \text{interstitial implant}$$

After N-doping by a substitutional or interstitial procedure, the electronic structure undergoes changes as can be seen in Fig. 7 (middle and top panels) where total and projected DOS for both configurations are reported in the most stable cases.

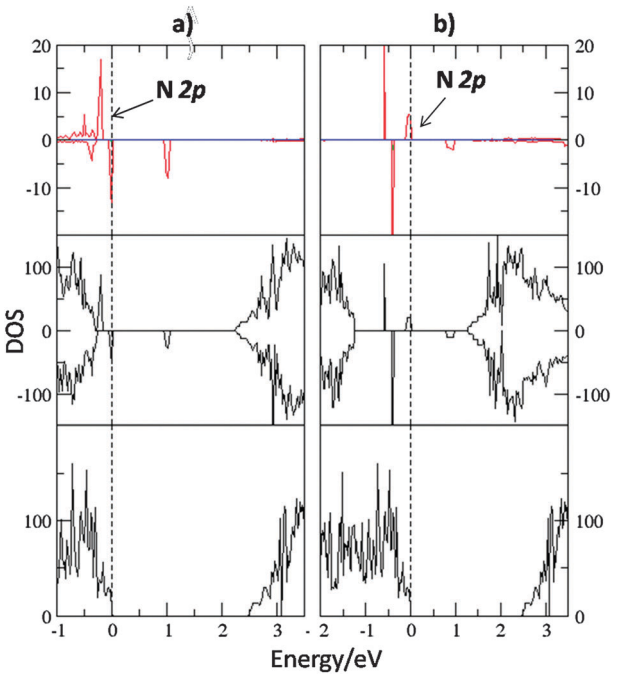

Fig. 7 DOS for (a) the N-doped TiO_2 for substitutional implant of nitrogen (b3b), and (b) the N-doped TiO_2 for interstitial implant of nitrogen (s2b_below). Top panels correspond to N projected states, middle panels the total DOS, and the bottom panels the TiO_2 total DOS. The Fermi level is at 0 eV.

The procedures to implant one nitrogen atom produce new states originated from the N 2p orbitals. The substitution of one oxygen atom by one nitrogen atom produces two new states near to the top of the valence band of the host and in the band gap (middle of Fig. 7a). The N electronic configuration is $1s^2 2s^2 2p^3$, therefore the empty states can trap the two electrons left by the removed oxygen atom in the substitutional implant, leading the nitrogen oxidation state to N^{-2}. So that, still there is an electronic empty state in the gap that can be clearly seen in the DOS projected on N (top of Fig. 7a). On the other hand, for interstitial implant (middle of Fig. 7b) the adsorbed nitrogen atom introduces new states, three close to the Fermi level, and also one electronic unoccupied orbital in the gap; which can be clearly observed in the DOS (top of Fig. 7b). The Bader charges were calculated for the two systems obtaining −0.89 (b3b), −1.03 (s2b) and −0.30 (s2b_below) $|e|$ for substitutional and interstitial implantation, respectively. It confirms that in the former the nitrogen atom gains more electrons than in the last one, where N–O covalent bound was found.

After the N-doping procedure, Au adsorption and O vacancy creation on the surface, the electronic structure undergoes deep changes. This rearrangement is schematized in Fig. 8 for both interstitial and substitutional implants. When a gold atom is deposited on the surface, the Au 6s orbital appears to be unoccupied, since there is an electron transfer from the Au 6s level, initially lying between the O 2p and Ti 3d bands,

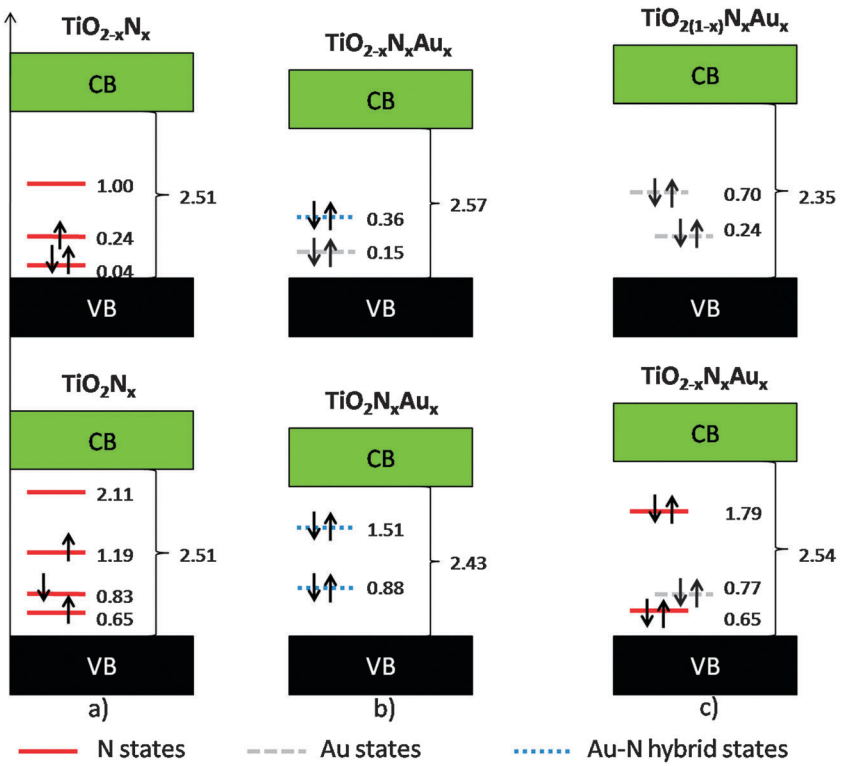

Fig. 8 Schematic representation of the orbital rearrangement in the most stable configurations after (a) implantation of nitrogen, (b) deposition of the gold atom to the previous system, and (c) creation of an oxygen vacancy in the preceding system. Top panels correspond to the substitutional implant of nitrogen, while bottom panels correspond to the interstitial implant of nitrogen. Thus, top (a), (b) and (c) are b3b, b3b-Ti1p1 and b3b-Ti1p1-s2b structures, respectively; though bottom (a), (b) and (c) are s2b_below, s2b_below-topN and s2b_below-topN-s2b structures, respectively.

towards the N 2p empty states. In the case that one nitrogen atom substitutes one oxygen atom, the process might be formally represented as:

$$TiO_{2-x}N_x^{2-} + Au^0 \rightarrow Au^+/TiO_{2-x}N_x^{3-}.$$

The initially empty N 2p state is now fully occupied, leading to a N atom with a closed shell, as schematized in top of Fig. 8b. On the other hand, after gold is deposited on the interstitial N-doped surface, the N 2p becomes partially occupied, where Au shows some s–p–d hybridization that improves the overlap with the N 2p orbitals, revealing some covalent contribution to the Au–N interaction (bottom of Fig. 8b).

In the case that Au atoms are deposited far from the N atom (b3b-Ti1p1), such a contribution is no longer observed in the DOS (not shown), although the electron transfer from Au to N still works as confirmed by the Bader analysis. Thus, the charges estimated in s2b-topN (contact) and b3b-Ti1p1 (no contact) models are 0.34, 0.46 for gold atoms, and −1.12 and −1.30 $|e|$ for N atoms, respectively. In other words, the electron transfer is not a localized mechanism and hence the adsorbed Au exhibits a cationic state oxidation in any of the considered configurations. On the other hand, this ionic character explains why gold atoms prefer to interact with anions (O^{2-} o N^{3-}) rather than to Ti^{4+} centers. However, the highest interaction is reached when the pair Au^+–N^{3-} is formed (s2b-topN), indicating that besides the electron transfer, ionic and covalent contributions are present and contribute to the stabilization of the system.

The creation of a vacancy in the Au^+/TiO_2N^{3-} introduces two more electrons in the systems that go to the impurity empty states. In the case of substitutional N-doping way the Au becomes a closed shell atom (top of Fig. 8c), while in the interstitial mode the 2p of nitrogen will be fully occupied (bottom of Fig. 8c). In both situations, the electron shift is accompanied by a migration of the gold atom to occupy the vacancy position.

The Bader analysis of gold/nitrogen atoms gives the values of −0.44/−1.28 and −0.40/−1.54 $|e|$ for b3b-Ti1p1-s2b and s2b_below-topN-s2b, respectively, confirming that gold and nitrogen atoms are negatively charged. This anionic state explains the larger stability of the configurations in which the gold atom interacts with the cations of the surface, specifically the adsorption at vacancy sites, where gold binds to the nearest Ti atoms. This result here found for anatase agrees with the trends observed for rutile in a previous work.[33]

It is well known that GGA approximation does not take into account the complete cancellation of the self-interaction by using any of the GGA exchange/correlation proposed functionals. One of the forms to study this kind of systems, where the localized density on Ti (3d) is crucial, can be done by using the GGA + U approach.[44] In this work, GGA + U approximation (U = 5.5 eV)[45] was used to perform a second optimization of the lowest energy structure b3b-Ti1p1-s2b. Only small differences are observed in the GGA and GGA + U relaxed structures. The largest changes are increments in the Au–Ti and N–Ti shortest bonds by 0.04 angstroms. After the GGA + U relaxation, the DOS was obtained and compared to the case of using the GGA functional (Fig. 9). It is observed that no new peaks are shaped in

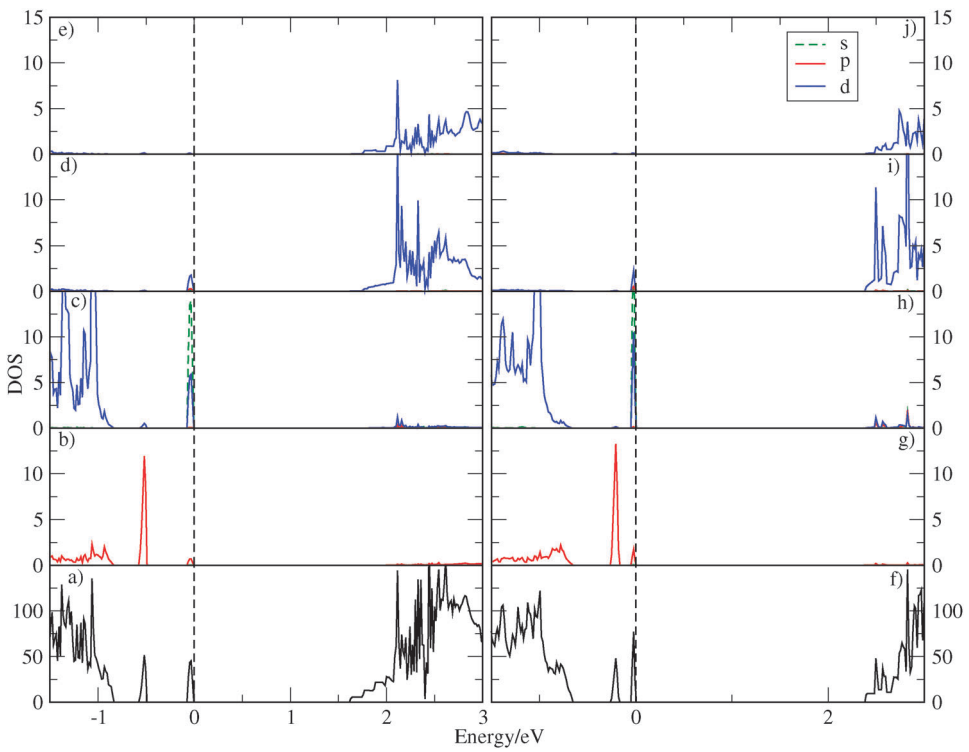

Fig. 9 DOS for the b3b-Ti1p1-s2b structure. GGA approximation was used to obtain the curves on the left panels, while GGA + U approximation was used for the right panels. The curves correspond to: total DOS (a and f), projected on a nitrogen atom (b and g), projected on a gold atom (c and h), projected on a titanium atom (Ti1 in Fig. 4d) close to the vacancy (d and i), and projected on a titanium atom (Ti2 in Fig. 4d) far from the vacancy (e and j).

the gap as a consequence of using GGA + U. The Bader charges on titanium atoms were also calculated by using both approximations and no relevant changes were obtained in the Ti atoms.

In the configuration b3b-Ti1p1-s2b, the Au atom occupies the site of the O vacancy, thus avoiding the polaronic defect states that are badly described by plain GGA.[59] In higher energy configurations where the vacancy site is unoccupied, the polaronic defect states may be badly reproduced by GGA. As the on-site Coulomb repulsion should increase further their energies, these states are not important in equilibrium situations.

In summary, we can conclude that in the absence of vacancies Au and N tend to be together. Since it is very difficult to get surfaces completely free from defects, Au will be likely trapped in the defects, while N will be as substitutional or interstitial. In any case, there is an electron transfer from Au to N when no oxygen vacancies are present ($Au^0 + N^{2-} \rightarrow Au^+ + N^{3-}$) and there is a double electron transfer when Au, N and vacancies are together ($V^{2-} + Au^0 + N^{2-} \rightarrow V^0 + Au^- + N^{3-}$) and, concomitantly, the oxygen vacancy will be occupied by Au. Finally, in the absence of vacancies, the configurations with Au and N in direct contact are preferred because an important covalent character is added to the electron transfer contribution.

4. Conclusions

In this work a theoretical study based on quantum mechanical DFT calculations has been performed on the (101) anatase surface in order to examine the effect of N-doping, the adsorption of the gold atom on the N-modified surface, and the effect of creation of oxygen vacancies in the system.

Substitutional and interstitial configurations for the N-doping have been considered, as well as, several adsorption sites for Au adatoms and different types of vacancies. Compared with the average error of PBE atomization energies (0.3 eV),[60] the energy differences between substitutionally N-doped configurations are rather small, and, therefore, the implantation could happen almost at any of the considered sites. Moreover, while subsurface substitutions are slightly favored over surface substitutions, the opposite trend is observed for interstitial N implantation, which is found to be favored at the outermost layer. In both modes, the implanted nitrogen atoms are quite unstable with respect to the possible formation of N_2. The N implantation modifies the electronic structure of TiO_2 and the DOS plots show the presence of N 2p localized filled states near the valence band edge and empty states in the middle of the band gap.

Gold atoms deposited on the N-modified surface prefer to bind at anionic sites, in particular close to N atoms. The analysis shows that the deposition is accompanied by a charge transfer from the gold toward nitrogen atom. Such electron transfer is found to happen even when gold and nitrogen are not in direct contact, although the highest interaction is observed when a pair Au–N is formed, where significant covalent contributions are also present. Furthermore, Au deposition also involves a small lowering in the surface band-gap, which is more visible in the interstitial case.

The presence of Au and N atoms at the surface makes it relatively easier the formation of oxygen vacancies as now the Au 6s orbitals might accommodate the excess of electrons in the Ti 3d band. These vacancies are most stable in the surface than in the subsurface as they are readily occupied by Au atoms that become negatively charged. Overall, the observed behavior is nearly analogous to that observed for the TiO_2(110) rutile surface which demonstrates that the synergism between implanted N, deposited Au atoms and vacancies does not qualitatively depend on the phase of the material.

Acknowledgements

This work was funded by the Ministerio de Ciencia e Innovación (Spain), grants MAT2008-04918 and CSD2008-00023. Computational resources were provided by the Centro Nacional de Supercomputación-Barcelona Supercomputing Center (Spain). N.C.H. and E.M.P. thank support from CONICYT (Chile) under Grants ACT/ADI24/2006 and ACI52/2008, the Junta de Andalucía (Incentivos 1/2006) and the Agencia Española de Cooperación Internacional (PCI/2006). We also thank Dr C. Di Valentin for helpful input to reproduce results of ref. 19.

References

1 U. Diebold, *Surf. Sci. Rep.*, 2003, **48**, 53–229.
2 A. L. Linsebigler, G. Lu and J. T. Yates, *Chem. Rev.*, 1995, **95**, 735–758.
3 K. I. Hadjiivanov and D. G. Klissurski, *Chem. Soc. Rev.*, 1996, **25**, 61–69.
4 B. O'Regan and M. Grätzel, *Nature*, 1991, **353**, 737–740.
5 A. Fujishima and K. Honda, *Nature*, 1972, **238**, 37–38.
6 H. Kato and A. Kudo, *J. Phys. Chem. B*, 2002, **106**, 5029–5034.
7 M. Haruta, *Catal. Today*, 1997, **36**, 153–166.
8 M. Haruta, N. Yamada, T. Kobayashi and S. Iijima, *J. Catal.*, 1989, **115**, 301–309.
9 R. Asahi, T. Morikawa, T. Ohwaki, K. Aoki and Y. Taga, *Science*, 2001, **293**, 269–271.
10 S. Sato, *Chem. Phys. Lett.*, 1986, **123**, 126–128.
11 A. Emeline, V. Kuznetsov, V. Rybchuk and N. Serpone, *Int. J. Photoenergy*, 2008, **2008**, 258394.
12 H. Irie, Y. Watanabe and K. Hashimoto, *J. Phys. Chem. B*, 2003, **107**, 5483–5486.
13 S. Na-Phattalung, M. F. Smith, K. Kim, M. Du, S. Wei, S. Zhang and S. Limpijumnong, *Phys. Rev. B: Condens. Matter Mater. Phys.*, 2006, **73**, 125205.
14 J. Y. Lee, J. Park and J. H. Cho, *Appl. Phys. Lett.*, 2005, **87**, 011904.
15 T. L. Thompson and J. T. Yates, *Chem. Rev.*, 2006, **106**, 4428–4453.
16 A. Vittadini and A. Selloni, *J. Chem. Phys.*, 2002, **117**, 353–361.
17 J. M. Herrmann, J. Disdier and P. Pichat, *Chem. Phys. Lett.*, 1984, **108**, 618–622.
18 C. Di Valentin, E. Finazzi, G. Pacchioni, A. Selloni, S. Livraghi, M. C. Paganini and E. Giamello, *Chem. Phys.*, 2007, **339**, 44–56.
19 E. Finazzi, C. Di Valentin, A. Selloni and G. Pacchioni, *J. Phys. Chem. C*, 2007, **111**, 9275–9282.
20 M. Batzill, E. Morales and U. Diebold, *Phys. Rev. Lett.*, 2006, **96**, 026103.
21 A. Nambu, J. Graciani, J. A. Rodriguez, Q. Wu, E. Fujita and J. F. Sanz, *J. Chem. Phys.*, 2006, **125**, 094706.
22 J. Graciani, L. J. Álvarez, J. A. Rodriguez and J. F. Sanz, *J. Phys. Chem. C*, 2008, **112**, 2624–2631.
23 J. Zhang, M. Zhang, Y. Han, W. Li, X. Meng and B. Zong, *J. Phys. Chem. C*, 2008, **112**, 19506–19515.

24 A. G. Thomas, W. R. Flavell, A. K. Mallick, A. R. Kumarasinghe, D. Tsoutsou, N. Khan, C. Chatwin, S. Rayner and G. Smith, *Phys. Rev. B: Condens. Matter Mater. Phys.*, 2007, **75**, 035105.
25 R. Sakthivel, T. Ntho, M. Witcomb and M. S. Scurrell, *Catal. Lett.*, 2009, **130**, 341–349.
26 M. Centeno, I. Carrizosa and J. A. Odriozola, *Appl. Catal., A*, 2003, **246**, 365–372.
27 M. Centeno, M. Paulis, M. Montes and J. A. Odriozola, *Appl. Catal., B*, 2005, **61**, 177–183.
28 B. Z. Tian, Ch. Li, F. Gu and H. Jiang, *Catal. Commun.*, 2009, **10**, 925–929.
29 M. S. Chen and D. M. Goodman, *Science*, 2004, **306**, 252–255.
30 N. C. Hernández, J. F. Sanz and J. A. Rodríguez, *J. Am. Chem. Soc.*, 2006, **128**, 15600–15601.
31 C. Arrouvel, M. Digne, M. Breysse, H. Toulhoat and P. Rayboud, *J. Catal.*, 2004, **222**, 152–166.
32 J. F. Sanz and N. C. Hernández, *Phys. Rev. Lett.*, 2005, **94**, 16104–16108.
33 J. Graciani, A. Nambu, J. Evans, J. A. Rodriguez and J. F. Sanz, *J. Am. Chem. Soc.*, 2008, **130**, 12056–12063.
34 G. Kresse and J. Hafner, *Phys. Rev. B: Condens. Matter*, 1993, **47**, 558–561.
35 G. Kresse and J. Furthmüller, *Comput. Mater. Sci.*, 1996, **6**, 15–50.
36 G. Kresse and J. Furthmüller, *Phys. Rev. B: Condens. Matter*, 1996, **54**, 11169–11186.
37 G. Kresse and D. Joubert, *Phys. Rev. B: Condens. Matter Mater. Phys.*, 1999, **59**, 1758–1775.
38 Y. Zhang and W. Yang, *Phys. Rev. Lett.*, 1998, **80**, 890–890.
39 J. P. Perdew, K. Burke and M. Ernzerhof, *Phys. Rev. Lett.*, 1998, **80**, 891–891.
40 J. K. Burdett, T. Hughbanks, G. J. Miller Jr., J. W. Richardson and J. V. Smith, *J. Am. Chem. Soc.*, 1987, **109**, 3639–3646.
41 H. I. Monkhorst and J. D. Pack, *Phys. Rev. B: Solid State*, 1976, **13**, 5188–5192.
42 P. E. Blöchl, O. Jepsen and O. K. Andersen, *Phys. Rev. B: Condens. Matter*, 1994, **49**, 16223–16233.
43 The DOS is projected onto spd atomic orbitals using the build in projector functions of the pseudopotentials (VASP option LORBIT = 10. Specification of a Wigner–Seitz radius is not needed) http://cms.mpi.univie.ac.at/vasp/vasp/vasp.html.
44 S. L. Dudarev, G. A. Botton, S. Y. Savrasov, C. J. Humphreys and A. P. Sutton, *Phys. Rev. B: Condens. Matter Mater. Phys.*, 1998, **57**, 1505–1509.
45 C. J. Calzado, N. C. Hernández and J. F. Sanz, *Phys. Rev. B: Condens. Matter Mater. Phys.*, 2008, **77**, 45118–45128.
46 C. T. Campbell, S. C. Parker and D. E. Starr, *Science*, 2002, **298**, 811–814.
47 C. G. Van de Wallea and J. Neugebauer, *J. Appl. Phys.*, 2004, **95**, 3851–3879.
48 K. Reuter and M. Scheffler, *Phys. Rev. B: Condens. Matter*, 2001, **65**, 35406–35417.
49 J. A. Rodriguez, T. Jirsak, G. Liu, J. Hrbek, J. Dvorak and A. Maiti, *J. Am. Chem. Soc.*, 2001, **123**, 9597–9605.
50 K. Jug, N. N. Fair and T. Bredow, *Phys. Chem. Chem. Phys.*, 2005, **7**, 2616–2621.
51 E. L. D. Hebenstreit, W. Hebenstreit, H. Geisler, C. A. Ventrice Jr., P. T. Sprunger and U. Diebold, *Surf. Sci.*, 2001, **486**, L467–L474.
52 J. Oviedo, M. A. San Miguel and J. F. Sanz, *J. Chem. Phys.*, 2004, **121**, 7427–7433.
53 H. Cheng and A. Selloni, *Phys. Rev. B: Condens. Matter Mater. Phys.*, 2009, **79**, 092101.
54 H. Chen, A. Nambu, W. Wen, J. Graciani, Z. Zhong, J. C. Hanson, E. Fujita and J. A. Rodríguez, *J. Phys. Chem. C*, 2007, **111**, 1366–1372.
55 C. Di Valentin, G. Pacchioni and A. Selloni, *Chem. Mater.*, 2005, **17**, 6656–6665.
56 R. Bader, *Atoms in Molecules: A Quantum Theory*, Clarendon Press, Oxford, 1990.
57 F. Labat, P. Baranek and C. Adamo, *J. Chem. Theory Comput.*, 2008, **4**, 341–352.
58 M. Ganduglia-Pirovano, A. Hofmann and J. Sauer, *Surf. Sci. Rep.*, 2007, **62**, 219–270.
59 G. Mattioli, P. Alippi, F. Filippone, R. Caminiti and A. A. Bonapasta, *J. Phys. Chem. C*, 2010, **114**, 21694–21704.
60 J. Perdew, K. Burke and M. Ernzerhof, *Phys. Rev. Lett.*, 1996, **77**, 3865–3868.

